Critical aspects of Raman spectroscopy as a tool for postmortem interval estimation.

Guillaume Falgayrac, Raffaele Vitale, Yann Delannoy, Helene Behal, Guillaume Penel, Ludovic Duponchel, Thomas Colard

Critical aspects of Raman spectroscopy as a tool for postmortem interval estimation

Guillaume Falgayrac[1*], Raffaele Vitale[2], Yann Delannoy[1], Hélène Behal[3], Guillaume Penel[1], Ludovic Duponchel[2], Thomas Colard[4,5]

Affiliations:

1 Univ. Lille, CHU Lille, Univ. Littoral Côte d'Opale, ULR 4490 - MABLab- Adiposité Médullaire et Os, F-59000 Lille, France

2 Univ. Lille, CNRS, UMR 8516 - LASIRE - Laboratoire Avancé de Spectroscopie pour les Intéractions la Réactivité et l'Environnement, F-59000 Lille, France

3 Univ. Lille, CHU Lille, ULR 2694 - METRICS: Évaluation des technologies de santé et des pratiques médicales, F-59000 Lille, France

4 Univ. Bordeaux, CNRS, MCC, PACEA, UMR 5199, F-33600 Pessac, France.

5 Department of Oral Radiology, University of Lille, Lille University Hospital, F-59000 Lille, France.

*Corresponding author: guillaume.falgayrac@univ-lille.fr

Guillaume FALGAYRAC

MABLab ULR4490

Faculty of Dentistry

Place de Verdun

59000 Lille FRANCE

Keywords: Raman spectroscopy, chemometrics, forensics, bone, ANOVA-simultaneous component analysis, burial

Abstract

The estimation of the postmortem interval (PMI) from skeletal remains represents a challenging task in forensic science. PMI is often influenced by extrinsic factors (humidity, dry, scavengers, etc.) and intrinsic factors (age, sex, pathology, way of life, medical treatments, etc.). Raman spectroscopy combined with multivariate data analysis represents a promising tool for forensic anthropologists. Despite all the advantages of the technique, Raman spectra of skeletal remains are influenced by these extrinsic and intrinsic factors, which impairs precision and reproducibility. Both parameters have to reach a high level of confidence when such spectroscopy is used as a way to predict PMI. As a consequence, advanced multivariate data analysis is necessary to quantify the effect of all factors to improve the estimation of the PMI.

The objective of this work is to evaluate the effect of intrinsic and extrinsic factors on the Raman spectra of skeletal remains. We designed a protocol close to a real-world scenario. We used ANOVA-simultaneous component analysis (ASCA) to unmix and quantify the effect of 1 intrinsic (source body) and 1 extrinsic (burial time) factors on the Raman spectra. In our model, the burial time (15.66%) was found to generate the highest variability after the source body (7.54%). ASCA showed that the variability due to the burial time has 2 mixed contributions. Seasonal variations are the first contribution. The second contribution is attributed to diagenesis. A decrease in the mineral band and an increase in the organic bands are observed. The source body was also found to contribute to the variability in Raman spectra. ASCA showed that the source body induces variability related to the composition of bone. This quantification cannot be assessed by basic chemometrics methods such as PCA. The results of this study highlighted the need to use an advanced chemometric data analysis tool (ASCA) combined with Raman spectroscopy to estimate the postmortem interval.

1 INTRODUCTION

Upon discovering skeletal remains, forensic anthropologists must answer several questions. These include determining the cause of death, identifying the deceased, and determining the postmortem interval (PMI). PMI corresponds to the delay between death and the discovery of the body. Thus, its estimation is a crucial part of forensic investigation. Beyond a certain PMI (which varies from country to country), a criminal investigation cannot be pursued. In France, the threshold is set at 20 years. Even if this estimation is a crucial step, forensic investigators do not have access to reliable and accurate methods at this time. Bell et al. called to strengthen the effort of scientific researchers and forensic doctors to improve forensic methods [1].

The estimation of the PMI from skeletal remains represents a challenging task in forensic medicine [2]. The PMI is often influenced by extrinsic factors (humidity, dry, scavengers, etc.) and intrinsic factors (age, sex, pathology, way of life, medical treatments, etc.). The existing methods involve the study of reactive molecules between bone and substrates [3-5], measurement of bone radioisotopes [6], and other physicochemical techniques [7-9]. Among these, vibrational spectroscopy (and particularly Raman spectroscopy) was found to yield satisfactory results in diverse application scenarios: it enabled the discrimination of forensic and archaeological remains [10], the differentiation of human and nonhuman bones [11], and the effect of diagenesis on bone molecular composition [12]. From these few examples, Raman spectroscopy represents a promising tool for forensic scientists with serious advantages. First, this spectroscopic analysis can be performed on a sample without preparation (or a few simple steps). Second, the technique simultaneously provides molecular information on the mineral and organic compounds in the bone. The last advantage is the nondestructive character of this analysis method. Indeed, the possibility of analyzing samples while preserving them is a real leitmotiv in forensic medicine. Handheld Raman spectroscopy devices are currently largely available on the market and constitute important resources for forensic investigators since they enable direct on-field operations [13].

Despite all the aforementioned pros, the global information encoded in a Raman spectrum can be considerably influenced by multiple factors at the same time, which often leads to scarce precision and reproducibility in the estimation of PMI values. Wang *et al*. highlighted this limitation in their study on human bone [2]. Creagh *et al*. used an animal

model to minimize these variations [14]. Mc Laughlin *et al*. stressed the need for advanced statistical methods for modeling the multiple sources of variation affecting vibrational spectroscopy data of bone samples [15]. Recent works considered the effect of intrinsic and seasonal factors in their approach but without the possibility of quantifying them from the data [16, 17]. More importantly, all attempts to use basic chemometric techniques such as principal component analysis (PCA) or partial least squares (PLS) regression without explicitly accounting for the effect of such factors resulted in suboptimal solutions [18].

In other scientific fields, such as metabolomics and food science, chemometricians have addressed the problem of disentangling these different sources of variation using an original multivariate data analysis approach called ANOVA-simultaneous component analysis (ASCA). ASCA combines the principles of both design of experiments (DoE) and multivariate exploratory analysis to evaluate whether a set of acquired data is significantly affected by specific experimental parameters (and/or interactions between them) and potentially quantify their effect on the measurements [19].

The objective of this work is to evaluate the effect of 1 intrinsic (source body) and 1 extrinsic factor (burial time) on the Raman spectra of skeletal remains. We designed an analytical protocol so as to get as close as possible to the real-world conditions observed during such a characterization. Then, the ASCA method was used to quantify the effect of the 2 factors and their interaction on the acquired Raman spectra.

2 MATERIAL AND METHODS

2.1 Samples

Six human subjects without known bone pathology were considered in this work (Table 1). All subjects were Caucasian and died of a heart attack. To comply with ethical standards, the analyzed bones were obtained from individuals who had "donated their bodies to science" according to a specific French law, which allows anatomic dissections and research to be performed on these human cadavers. Ribs were chosen for investigation given their importance in anthropology (e.g., estimating the age at death) [20, 21]. It was decided to work with fresh bone samples as embalming procedures induce changes in their molecular composition [22]. Moreover, the use of fresh ribs permits mimicking the conditions of a real-case scenario of discovery of skeletal remains.

Table 1: Characteristics of the subjects: 4 males and 2 females. Mean age of the group: 83.5 (± 7.1) year-old.

ID	Gender	Age	observations
#1	male	72	no records
#2	female	92	coxarthrosis, knee surgery, osteonecrosis of the femoral head
#3	female	80	heart prosthetic stent, vascular issues, Alzheimer's disease
#4	male	88	hypertension
#5	male	82	acute myeloid leukemia, alcoholism, smoker
#6	male	87	no records

The experimental protocol was designed as follows. For each subject, two ribs (R1 and R4) were harvested on the day of death. The flesh surrounding bones was mechanically removed without any further treatment. A 5-mm-long section of bone was cut transversally across each rib using a diamond saw. The bone section was then used for Raman microscopy. These samples represented the baseline (T0). The holes resulting from this preparatory step were then covered with neutral wax before the ribs were placed back in their burial environment. The latter procedure was repeated each month for 12 months. Each pair of ribs (R1 and R4) from the same subject was placed into its own tray (Figure 1a). Each plastic tray was filled with clay soil typical of northern France. The soil pH was 6.8 and described as brown to brown leached, low hydromorphic, aeolian silt on clay and sandy substrate of the Lille Region (Table 2). The ribs were covered by approximately 1 cm of soil (Figure 1b). Plastic trays were placed outside and under cover to protect them from scavengers and rain. This sampling method has been shown not to induce any change in the sample [23]. The local weather data were retrieved from the Metéo France website (Table 2).

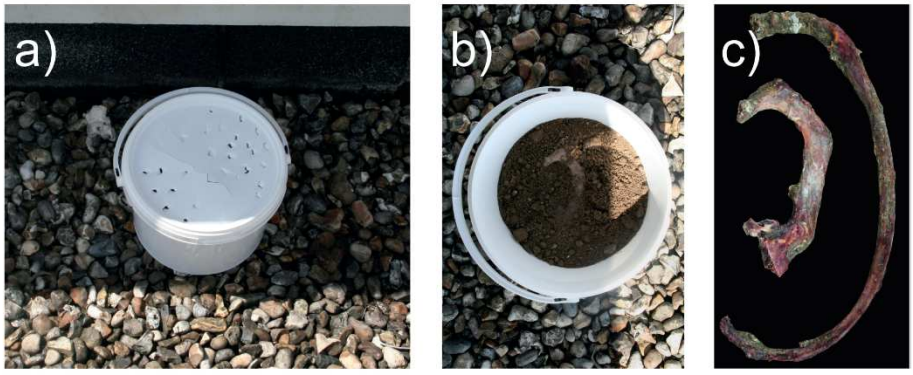

Figure 1: a) plastic tray with lid to protect from scavengers. The plastic tray was sheltered to protect from rain; b) plastic tray filled with clay soil typical of northern France carrying the rib; c) ribs n°1 and 4 after 1 month of burial time

Table 2: Features of the burial environments of the first and fourth ribs (labeled R1 and R4, respectively). For each subject, R1 and R4 ribs were placed on a soil surface and covered by an approximately 1 cm thin layer of soil.

	R1 and R4
Bone class	First and fourth right ribs
Environment	Outdoor
Environmental conditions	Under cover
Soil type/pH	Clay/6.8
Temperature range during the experiment (mean ±SD) in °C	T° mean: 10.5 ±4.7 T°max: 14.4 ±5.4 T°min: 7.0 ±4.2
Relative humidity (%)	79.5 ±6.8

2.2 Raman microspectrometry

Each 5-mm-long section of ribs was analyzed by Raman microspectroscopy every month for one year. The spectrometer was installed in a room with controlled temperature. Raman spectra were acquired with a LabRAM HR800 Raman microspectrometer (Jobin-Yvon, Villeneuve d'Ascq, France) equipped with DuoScan technology, an XYZ motorized stage, and a 785 nm laser diode [24]. A mean spectrum was acquired over a rastered bone area of 30 x 30 µm². The acquisition time was set to 30 s, considering a 300-1700 cm^{-1} spectral domain. Prior to spectroscopic acquisition, each 5-mm-long section was stuck on a microscope slide and polished with decreasing grain size (from 30 to 0.3 µm). For each rib, 4 specific zones were anatomically identified: secondary osteon, interstitial bone, periosteum, and trabecular bone. Ten spectra were acquired per anatomic zone, ultimately resulting in 40 spectra per rib per month. The 2 final sets of 40 spectral profiles per rib per month (max-normalized) were joint and averaged prior to further processing.

2.3 The proposed multivariate approach: ANOVA-simultaneous component analysis (ASCA)

ANOVA-simultaneous component analysis (ASCA) combines the advantages of both design of experiments and multivariate exploratory analysis to study whether the recorded data are

significantly affected by certain experimental parameters or factors (and/or by the interaction of multiple factors) and to assess how they actually vary under their influence [25, 26]. Let **X** be a two-dimensional data structure whose rows correspond to the Raman spectra collected and whose columns to the spectral channels sampled. Mathematically speaking, ASCA decomposes the centered data matrix ($\overline{\mathbf{X}}$) into the sum of several arrays according to the ANOVA scheme. In this work, the effects of the source body (Factor A) and the burial time (Factor B) on the evolution of the bone composition will be investigated. The partition of $\overline{\mathbf{X}}$ is carried out as:

$$\overline{\mathbf{X}} = \mathbf{X}_{\mathrm{A}} + \mathbf{X}_{\mathrm{B}} + \mathbf{X}_{\mathrm{AB}} + \mathbf{E} \quad (1)$$

where $\mathbf{X}_{\mathrm{A}}$, $\mathbf{X}_{\mathrm{B}}$ and $\mathbf{X}_{\mathrm{AB}}$ account for the variability induced by the effect of Factor A, Factor B and Factor A/Factor B interaction, respectively, while $\mathbf{E}$ carries the residuals not explained by the model.

To evaluate whether the effect of a factor/interaction on the data variation is statistically significant, the sum-of-squares of the corresponding submatrix is computed as in Eq. 2:

$$SSQ_i = ||\mathbf{X}_i||^2 \; \forall \; i = \{\mathrm{A}, \mathrm{B}, \mathrm{AB}\} \quad (2)$$

with $\| \ \|^2$ denoting the Euclidean norm. SSQ_i is afterward contrasted against a *null* distribution nonparametrically estimated by permutation testing conducted on the residuals of the so-called *reduced model* (*i.e.*, by shuffling the rows of the augmented matrix obtained by summing the sub-array related to the specific factor or interaction under study and $\mathbf{E}$) [27, 28]. If the observed sum-of-squares is found to be systematically larger than the values of such a *null* distribution (*p value*<0.05), the tested effect is then assumed to be statistically significant and $\mathbf{X}_i$ decomposed by simultaneous component analysis (SCA) as:

$$\mathbf{X}_i = \mathbf{T}_i \mathbf{P}_i^{\mathrm{T}} \quad (3)$$

where $\mathbf{T}_i$ and $\mathbf{P}_i$ **are** the scores and the loadings matrices resulting from a principal component analysis (PCA) model constructed under the ANOVA scheme constraint. The graphical representation of $\mathbf{T}_i$ and $\mathbf{P}_i$ provides direct insights into the data variability induced by the concerned factor/interaction.

From a technical perspective, according to the theory of design of experiments, factor A and factor B have a different inherent nature: the former is defined as random, while factor B can be considered as fixed. In principle, random factors cannot be readily coped with by the classical implementation of ASCA, which is capable of directly handling only fixed ones. Nonetheless, in statistics, it is rather common to fit random factors as fixed especially when the amount of levels spanned (here, the number of source bodies) is limited or the distributional assumptions that need to be fulfilled for modelling random factors as such do not necessarily hold (this happens, for example, if they are associated to relatively strong effects and/or their levels are not drawn from a homogeneous population, as is to be expected in this particular case-study) [29, 30]. For this reason, for the sake of simplicity and in the light of the fact that virtually identical results were obtained by means of an alternative approach that preserves the *randomness* of factor B (*i.e.*, repeated measures ASCA+ [31] – not shown), only the outcomes returned by standard ASCA will be discussed in the following sections.

3 Results

3.1 The extrinsic and intrinsic factors have a significant contribution to the data variability

A classical PCA was applied to the original spectral dataset, but no clear separation of the samples according to their corresponding burial time was found (data not shown). This is representative of the presence of multiple sources of variation (intrinsic and extrinsic factors) simultaneously affecting the data and potentially masking those of interest [11, 18]. ASCA was applied to take into account the effect of these factors. One intrinsic and one extrinsic factors were considered: the subject (from 1 to 6) and the burial time (from baseline to 12 months). These factors were modeled separately to quantify their effect on the Raman spectra. Permutation tests were exploited to test the effect of these two factors and their binary interaction on the variation of the collected Raman spectra. Table 3 summarizes the results obtained after 1000 permutations.

Table 3: Summary of the ASCA results. The percentage of variance explained is calculated with respect to the mean-centered data, $\overline{X}$. Results obtained after 1000 permutations.

Factor/interaction	Factor/interaction array	*p value*	Variance explained (%)
Source body	$\mathbf{X}_{\mathrm{A}}$	<0.001	7.54%
Burial time	$\mathbf{X}_{\mathrm{B}}$	<0.001	15.66%
Source body/burial Time	$\mathbf{X}_{\mathrm{AB}}$	<0.001	56.79%

The two main factors (*i.e.*, source body and burial time) as well as the binary interaction source body/burial time were found to have a statistically significant influence on the recorded measurements. $\mathbf{X}_{\mathrm{A}}$, $\mathbf{X}_{\mathrm{B}}$ and $\mathbf{X}_{\mathrm{AB}}$ were therefore decomposed as in Equation 3 for a visual inspection of such induced changes. More specifically, to better differentiate the samples characterized at the distinct levels of each factor/interaction, SCA scores accounting for within-level variability were estimated as [32]:

$$\mathbf{T}_{(\mathbf{X}_i+\mathbf{E})} = (\mathbf{X}_i + \mathbf{E})\mathbf{P}_i \quad (4)$$

In addition, to enable a more straightforward interpretation of the final ASCA model, the corresponding loadings were subjected to a statistical bootstrapping procedure that permitted to readily identify the spectral features mainly responsible for the observed differences [31, 33-35]. This procedure encompasses two sequential algorithmic steps (iterated 1000 times): first, bootstrapping with substitution is carried out on a random number of raw spectral profiles within each individual level of the simple factors or binary interaction under study. Afterwards, the resulting data matrix is decomposed according to the same ASCA model built on the original one. It is important to notice here that, as slightly different versions of the initial data array are repeatedly analyzed, the ASCA loadings retrieved at each bootstrapping iteration need to be rotated with respect to some common reference profiles. In this particular case, such loadings were orthogonal Procrustes-rotated towards those extracted from the non-bootstrapped data.

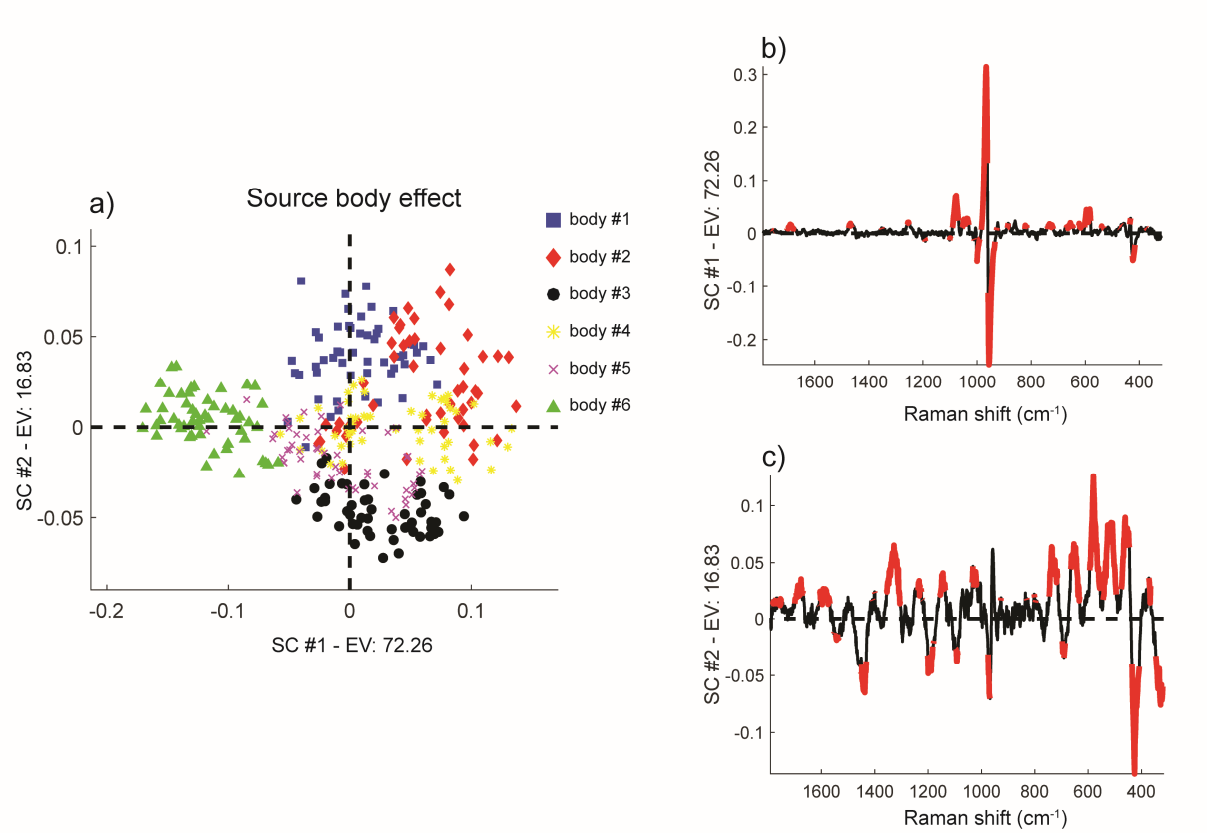

Figure 2 represents the outcomes yielded by the decomposition of $\mathbf{X}_A$ (source body effect)[1]. Scores clearly clustered according to the source body index along the first and second simultaneous components (SCs) (Figure 2a). The SC#1 loadings are characterized by an intense band at 960 cm^{-1} assigned to phosphate vibration (v_1PO_4) and a minor band at 1070 cm^{-1} assigned to carbonate vibration (v_1CO_3). The SC#2 loadings are characterized by Raman bands assigned to the organic and mineral matrix: 1670 cm^{-1} (amide I), 1450 cm^{-1} (CH_2 collagen type I), 1260 cm^{-1} (amide III), 590 cm^{-1} (v_4PO_4) and 430 cm^{-1} (v_2PO_4).

[1] For every factor/interaction effect matrix, the lowest number of components explaining approximately 90% of its variance was extracted.

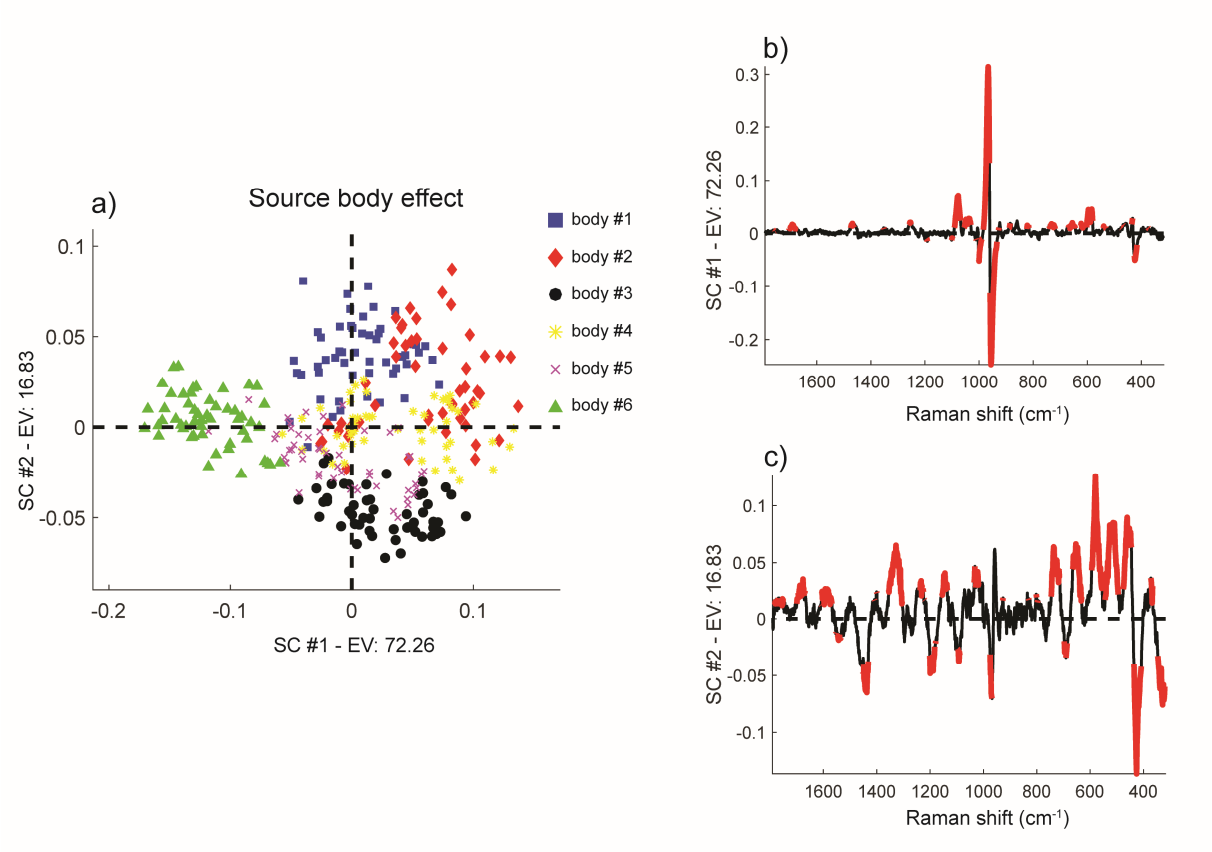

Figure 2: a) X_A SC1 vs. SC2 scores plot. Legend: body #1 (blue squares); body #2 (red diamonds); body #3 (black circles); body #4 (yellow stars); body #5 (magenta crosses); body #6 (green triangles). X_A loadings profiles along b) SC1 and c) SC2. Loading values found to be either always positive or always negative across 1000 bootstrapping iterations and, therefore, associated with wavelength channels relevant for the sake of interpretation are highlighted in red. SC and EV stand for simultaneous component and explained variance, respectively.

Figure 3 shows the output of the ASCA analysis for $\mathbf{X}_B$ (burial time). The scores along SC#1 (Figure 3a) follow a sinusoidal temporal trend. The outlying behavior noticeable at months 8 and 9 is due to a power failure of the laser, which was replaced at month 10. The SC#1 loadings are characterized by a strong contribution at 960 cm^{-1}. The scores along SC#2 decrease continuously as a function of burial time. Positive scores are observed for spectra collected between 0 and 5 months, and negative scores are observed for spectra collected between 5 and 12 months. Positive and negative loadings are found for mineral and organic bands, respectively.

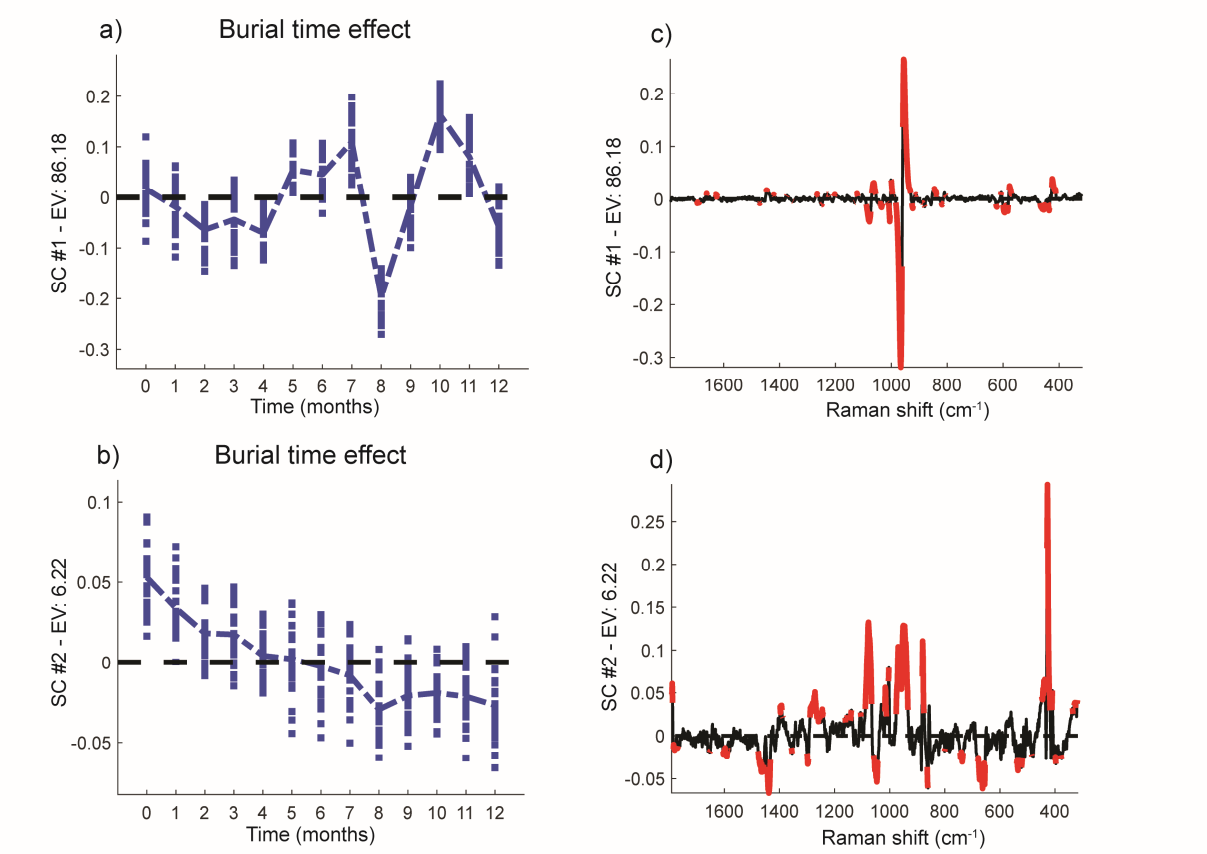

Figure 3: Longitudinal plots of the a) first and b) second X_B SC scores. Here, each sample at each month is represented as a blue square. The dashed line connects the mean scores values calculated at the different time steps. X_B loadings profiles along c) SC1 and d) SC2. Loading values found to be either always positive or always negative across 1000 bootstrapping iterations and, therefore, associated with wavelength channels relevant for the sake of interpretation are highlighted in red. SC and EV stand for simultaneous component and explained variance, respectively.

3.2 The interaction "PMI+body/PMI" interactions

In the last step and as recommended in previous works, SCA was performed on $(\mathbf{X}_{\mathrm{B}} + \mathbf{X}_{\mathrm{AB}})$ to more systematically explore the effect of the binary interaction source body/burial time [34, 35]. In this regard, both the SC#1 and SC#2 longitudinal scores plots in Figure 4a and 4b show profiles fluctuating (with different frequencies) and substantially shifting in time for the concerned six source bodies. The largest contributions to these two components are given by the Raman band centered at 960 cm^{-1} and by the mineral and organic bands attributed beforehand, respectively.

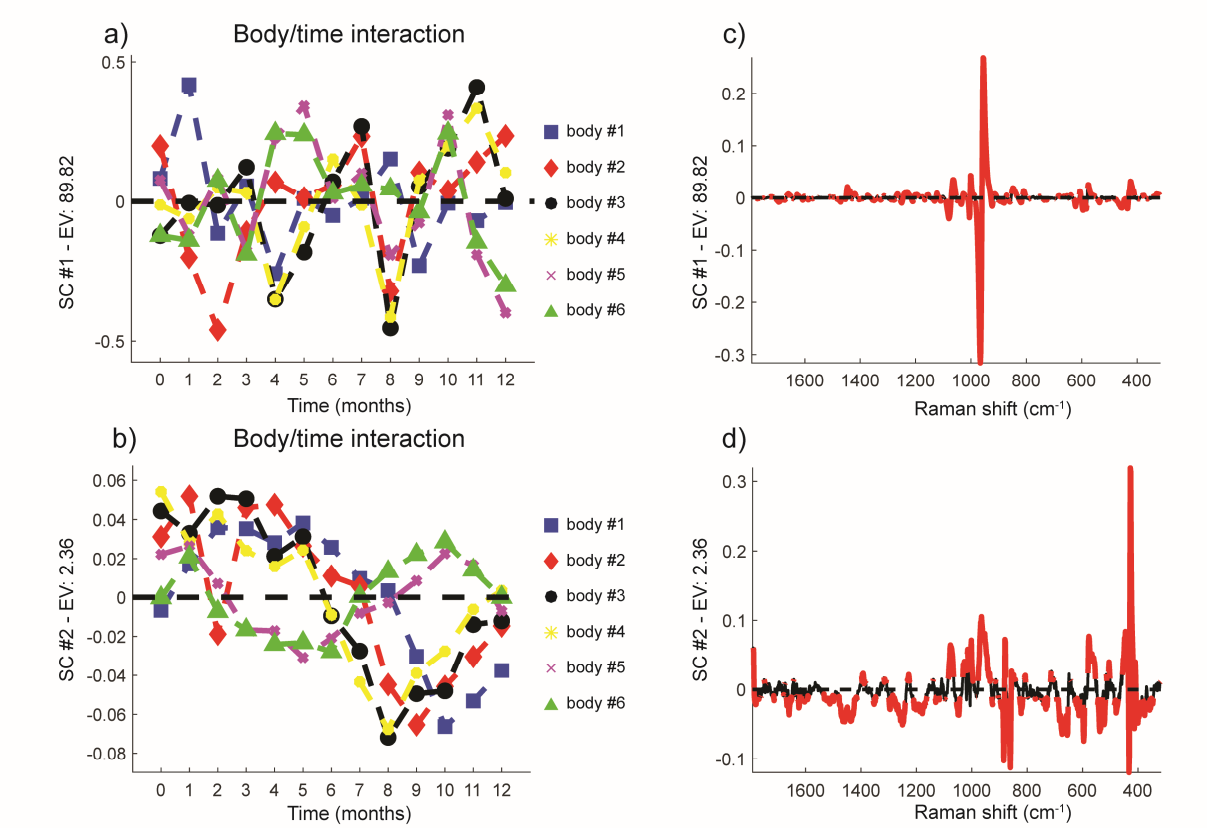

Figure 4: Longitudinal plots of the a) first and b) second $(X_B + X_{AB})$ SC scores. Here, each sample at each burial time point is represented as a symbol of a different color; body #1 (blue squares); body #2 (red diamonds); body #3 (black circles); body #4 (yellow stars); body #5 (magenta crosses); body #6 (green triangles). The dashed lines connect the mean scores values calculated at the different time steps for each source body (line colors are coherent with those of the corresponding symbols). $(X_B + X_{AB})$ loadings profiles along c) SC1 and d) SC2. Loading values found to be either always positive or always negative across 1000 bootstrapping iterations and, therefore, associated with wavelength channels relevant for the sake of interpretation are highlighted in red. SC and EV stand for simultaneous component and explained variance, respectively.

4 Discussion

In the last 5 years, various studies have been published to establish a proof-of-concept about the use of vibrational spectroscopy to analyze bones in the forensic field. Each study addresses specific questions: comparison of techniques of analysis [36, 37]; comparison of chemometric methods [2]; differentiation of archeologic *vs* forensic bones [10]; diagenesis of burned bones [38]; estimation of the PMI [16]; and use of animal bones as a human proxy [11]. Most of the studies used infrared spectroscopy (FTIRM, IR reflexion, ATR, or MIR) to a much lesser extent than Raman microspectroscopy. All studies agree that vibrational techniques are suitable for forensic investigation. However, there are still issues to overcome to make vibrational techniques ready-to-use for forensic investigators. One recurrence is the influence of intrinsic and extrinsic factors on the infrared and Raman spectra of bones. This

issue, commonly highlighted in previous studies, impairs precision and reproducibility [2, 14-16, 18]. These studies employed chemometric techniques such as principal component analysis (PCA), partial least square (PLS) regression, or genetic algorithms. The precision and reproducibility were improved by the chemometric approach compared to univariate analysis. PCA is commonly used to highlight spectral differences between datasets from 2 specific conditions. PCA revealed differences between groups when one condition was tested and other factors remained equivalent. However, in the situation of a follow-up of degradation of bones in their environment, there are extrinsic and intrinsic factors that represent different sources of spectral variation. PCA is not able to make the difference between all the sources of variations as it does not directly account for their effect, which resulted in a limited improvement.

Based on these observations, the objective of this study was to critically evaluate Raman spectroscopy as a tool for estimating the burial time by considering the effect of one intrinsic and one extrinsic factor. We designed a protocol close to a real-world scenario. We used an advanced multivariate method (ASCA) to separate and quantify the effects of these factors (body and burial time) on the Raman spectra. We quantified these effects on the variability of the considered dataset. In our model, the effect was ranked as follows: burial time (15.66%) > source body (7.54%).

The first factor, “burial time” (extrinsic factor), represents the highest variability, explaining 15.66% compared to the other. Among these 15.66%, the ASCA analysis revealed 2 contributions. The scores of SC#1 follow a sinusoidal trend within 12 months of burial time and represent 86.18% of the variance explained. This sinusoidal trend is likely caused by yearly seasonal fluctuations even in a room with controlled temperature. This result suggests that yearly variations might not be related to room temperature but to another factor that is difficult to identify with this protocol. The scores of SC#2 follow a decreasing trend within 12 months of burial time and represent 6.22% of the variance explained. SC#2 accounts for a decrease in the Raman intensity of the mineral bands and an increase in the Raman intensity of the organic bands over burial time. The decrease in mineral bands and the increase in organic bands suggest a decrease in the mineral/organic ratio parameter. This parameter was also found to decrease when the burial period was less than 24 months in an animal model [14, 15]. The use of advanced chemometrics methods is strongly recommended in the light of

these results. The low contribution of the burial time to the variability could explain the absence of clustering on the PCA results.

The intrinsic factor considered was the source body which accounted for 7.54% of the total variability observed. Among the 7.54%, ASCA detected 2 main contributions. SC#1 (72.26%) relates to mineral bands, and SC#2 (16.83%) to organic bands. These results indicate that bone samples show characteristic spectroscopic signatures depending on the subject; therefore, the bone composition varies among subjects. Such a variation is related to interindividual differences and may have multiple origins: gender [39], age [40, 41], drugs [42], pathologies [43], food intake [44], and so on. Therefore, with the aim of using Raman spectroscopy as a tool for estimating the burial time, the variability associated with the subject's history should be taken into account. In our model, it accounts for 7.54% of the explained variance (half of the effect of the burial time). It represents anyway a significant source of variation which can lead to an error in the estimation of the burial time.

This study has limitations related to the investigation of human samples. First, the study was performed with a limited number of subjects (n=6). The number of samples was limited due to the accessibility of fresh human samples. The authors excluded bone samples that were fixed by any protocol because it modifies the composition of bone [22, 45]. Second, bone samples were obtained from old subjects. The inclusion of younger subjects would have been a serious constraint within the timeframe of the study.

5 Conclusion

The objective of this work was to evaluate the effect of environmental factors on the Raman spectra of skeletal remains. The effect of two factors (source body and burial time) and their binary interaction on the variability of the spectral profiles was quantified and assessed. Our approach provides a clear overview of how Raman bands evolve under the action of every single factor/interaction. In our experimental design, the burial time and the source body had a significant contribution to the variability of the collected data. From a forensic point of view, the results of this study show that (i) an advanced chemometric data analysis tool (ASCA) is needed when attempting to use Raman spectroscopy for the estimation of PMI and (ii) the intrinsic factor "source body" may alter the estimation of the PMI.

6 Authors contribution

Y.D., T.C., G.F., G.P. designed the research. Y.D., G.F. performed research. Y.D acquired data. L.D., R.V., H.B. performed the statistical analysis. Y.D., T.C., G.F, G.P., L.D., R.V. interpreted the data. Y.D., T.C., G.F, L.D., R.V. wrote the paper. All authors read and approved the paper.

7 Acknowledgements

The authors thanks Olivier Devos for his precious advices at the beginning of the study.

8 References

[1] S. Bell, S. Sah, T.D. Albright, S.J. Gates, Jr., M.B. Denton, A. Casadevall, A call for more science in forensic science, Proc. Natl. Acad. Sci. U. S. A. 115(18) (2018) 4541-4544.
[2] Q. Wang, Y. Zhang, H. Lin, S. Zha, R. Fang, X. Wei, S. Fan, Z. Wang, Estimation of the late postmortem interval using FTIR spectroscopy and chemometrics in human skeletal remains, Forensic Sci. Int. 281 (2017) 113-120.
[3] S. Berg, The determination of bone age, Methods of forensic science, vol. 21963, pp. 231-252.
[4] F. Ramsthaler, S.C. Ebach, C.G. Birngruber, M.A. Verhoff, Postmortem interval of skeletal remains through the detection of intraosseal hemin traces. A comparison of UV-fluorescence, luminol, Hexagon-OBTI(R), and Combur(R) tests, Forensic Sci. Int. 209(1-3) (2011) 59-63.
[5] J.M. Very, R. Gibert, B. Guilhot, M. Debout, C. Alexandre, Effect of aging on the amide group of bone matrix, measured by FTIR spectrophotometry, in adult subjects deceased as a result of violent death, Calcif. Tissue Int. 60(3) (1997) 271-5.
[6] B. Swift, I. Lauder, S. Black, J. Norris, An estimation of the post-mortem interval in human skeletal remains: a radionuclide and trace element approach, Forensic Sci. Int. 117(1-2) (2001) 73-87.
[7] M.A. Brown, A.W. Bunch, C. Froome, R. Gerling, S. Hennessy, J. Ellison, Citrate Content of Bone as a Measure of Postmortem Interval: An External Validation Study, J. Forensic Sci. 63(5) (2018) 1479-1485.
[8] M.A. Castellano, E.C. Villanueva, R. von Frenckel, Estimating the date of bone remains: a multivariate study, J. Forensic Sci. 29(2) (1984) 527-34.
[9] K. Johnsson, Chemical Dating of Bones Based on Diagenetic Changes in Bone Apatite, Journal of Archaeological Science 24 (1997) 431-437.
[10] T. Leskovar, I. Zupanic Pajnic, I. Jerman, M. Cresnar, Separating forensic, WWII, and archaeological human skeletal remains using ATR-FTIR spectra, Int. J. Legal Med. (2019).
[11] Q. Wang, W. Li, R. Liu, K. Zhang, H. Zhang, S. Fan, Z. Wang, Human and non-human bone identification using FTIR spectroscopy, Int. J. Legal Med. 133(1) (2019) 269-276.
[12] G. Dal Sasso, I. Angelini, L. Maritan, G. Artioli, Raman hyperspectral imaging as an effective and highly informative tool to study the diagenetic alteration of fossil bones, Talanta 179 (2018) 167-176.
[13] W.R. de Araujo, T.M.G. Cardoso, R.G. da Rocha, M.H.P. Santana, R.A.A. Munoz, E.M. Richter, T. Paixao, W.K.T. Coltro, Portable analytical platforms for forensic chemistry: A review, Anal. Chim. Acta 1034 (2018) 1-21.
[14] D. Creagh, A. Cameron, Estimating the Post-Mortem Interval of skeletonized remains: The use of Infrared spectroscopy and Raman spectro-microscopy, Radiat Phys Chem 137 (2017) 225-229.
[15] G. McLaughlin, I.K. Lednev, Potential application of Raman spectroscopy for determining burial duration of skeletal remains, Anal. Bioanal. Chem. 401(8) (2011) 2511-8.
[16] A. Baptista, M. Pedrosa, F. Curate, M.T. Ferreira, M.P.M. Marques, Estimation of the post-mortem interval in human bones by infrared spectroscopy, Int. J. Legal Med. 136(1) (2022) 309-317.

[17] P.S. Garagoda Arachchige, J.L. Hughes, L.S. Bell, K.C. Gordon, S.J. Fraser‐Miller, Detection of structural degradation of porcine bone in different marine environments with Raman spectroscopy combined with chemometrics, J. Raman Spectrosc. (2021).
[18] L. Ortiz-Herrero, B. Uribe, L.H. Armas, M.L. Alonso, A. Sarmiento, J. Irurita, R.M. Alonso, M.I. Maguregui, F. Etxeberria, L. Bartolome, Estimation of the post-mortem interval of human skeletal remains using Raman spectroscopy and chemometrics, Forensic Sci. Int. 329 (2021) 111087.
[19] C. Bertinetto, J. Engel, J. Jansen, ANOVA simultaneous component analysis: A tutorial review, Anal Chim Acta X 6 (2020) 100061.
[20] K. Zhang, F. Fan, M. Tu, J.-H. Cui, J.-S. Li, Z. Peng, Z.-H. Deng, The role of multislice computed tomography of the costal cartilage in adult age estimation, Int. J. Legal Med. 132(3) (2018) 791-798.
[21] M. Partido Navadijo, I. Fombuena Zapata, E.A. Borja Miranda, I. Alemán Aguilera, Discriminant functions for sex estimation using the rib necks in a Spanish population, Int. J. Legal Med. 135(3) (2021) 1055-1065.
[22] T. Pascart, B. Cortet, C. Olejnik, J. Paccou, H. Migaud, A. Cotten, Y. Delannoy, A. During, P. Hardouin, G. Penel, G. Falgayrac, Bone Samples Extracted from Embalmed Subjects Are Not Appropriate for the Assessment of Bone Quality at the Molecular Level Using Raman Spectroscopy, Anal. Chem. 88(5) (2016) 2777-83.
[23] R.E. Adlam, T. Simmons, The effect of repeated physical disturbance on soft tissue decomposition--are taphonomic studies an accurate reflection of decomposition?, J. Forensic Sci. 52(5) (2007) 1007-14.
[24] G. Falgayrac, B. Cortet, O. Devos, J. Barbillat, V. Pansini, A. Cotten, G. Pasquier, H. Migaud, G. Penel, Comparison of two-dimensional fast Raman imaging versus point-by-point acquisition mode for human bone characterization, Anal. Chem. 84(21) (2012) 9116-23.
[25] J.J. Jansen, H.C.J. Hoefsloot, J. Van Der Greef, M.E. Timmerman, J.A. Westerhuis, A.K. Smilde, ASCA: analysis of multivariate data obtained from an experimental design, Journal of Chemometrics 19(9) (2005) 469-481.
[26] A.K. Smilde, J.J. Jansen, H.C.J. Hoefsloot, R.-J.A.N. Lamers, J. Van Der Greef, M.E. Timmerman, ANOVA-simultaneous component analysis (ASCA): a new tool for analyzing designed metabolomics data, Bioinformatics 21(13) (2005) 3043-3048.
[27] M. Anderson, C.T. Braak, Permutation tests for multi-factorial analysis of variance, Journal of Statistical Computation and Simulation 73(2) (2003) 85-113.
[28] D.J. Vis, J.A. Westerhuis, A.K. Smilde, J. Van Der Greef, Statistical validation of megavariate effects in ASCA, BMC Bioinformatics 8(1) (2007) 322.
[29] J. Camacho, C. Díaz, P. Sánchez‐Rovira, Permutation tests for ASCA in multivariate longitudinal intervention studies, Journal of Chemometrics (2022).
[30] H. Schielzeth, S. Nakagawa, Nested by design: model fitting and interpretation in a mixed model era, Methods Ecol. Evol. 4(1) (2013) 14-24.
[31] T.S. Madssen, G.F. Giskeodegard, A.K. Smilde, J.A. Westerhuis, Repeated measures ASCA+ for analysis of longitudinal intervention studies with multivariate outcome data, PLoS Comput. Biol. 17(11) (2021) e1009585.
[32] G. Zwanenburg, H.C.J. Hoefsloot, J.A. Westerhuis, J.J. Jansen, A.K. Smilde, ANOVA-principal component analysis and ANOVA-simultaneous component analysis: a comparison, Journal of Chemometrics 25(10) (2011) 561-567.

[33] M. Bevilacqua, R. Bucci, S. Materazzi, F. Marini, Application of near infrared (NIR) spectroscopy coupled to chemometrics for dried egg-pasta characterization and egg content quantification, Food Chem. 140(4) (2013) 726-34.
[34] P. Firmani, R. Vitale, C. Ruckebusch, F. Marini, ANOVA-Simultaneous Component analysis modelling of low-level-fused spectroscopic data: A food chemistry case-study, Anal. Chim. Acta 1125 (2020) 308-314.
[35] S. De Luca, M. De Filippis, R. Bucci, A.D. Magrì, A.L. Magrì, F. Marini, Characterization of the effects of different roasting conditions on coffee samples of different geographical origins by HPLC-DAD, NIR and chemometrics, Microchem. J. 129 (2016) 348-361.
[36] A. Amadasi, A. Cappella, C. Cattaneo, P. Cofrancesco, L. Cucca, D. Merli, C. Milanese, A. Pinto, A. Profumo, V. Scarpulla, E. Sguazza, Determination of the post mortem interval in skeletal remains by the comparative use of different physico-chemical methods: Are they reliable as an alternative to (14)C?, Homo 68(3) (2017) 213-221.
[37] S. Longato, C. Wöss, P. Hatzer-Grubwieser, C. Bauer, W. Parson, S.H. Unterberger, V. Kuhn, N. Pemberger, A.K. Pallua, W. Recheis, R. Lackner, R. Stalder, J.D. Pallua, Post-mortem interval estimation of human skeletal remains by micro-computed tomography, mid-infrared microscopic imaging and energy dispersive X-ray mapping, Analytical Methods 7(7) (2015) 2917-2927.
[38] M.P.M. Marques, A.P. Mamede, A.R. Vassalo, C. Makhoul, E. Cunha, D. Goncalves, S.F. Parker, L.A.E. Batista de Carvalho, Heat-induced Bone Diagenesis Probed by Vibrational Spectroscopy, Sci. Rep. 8(1) (2018) 15935.
[39] N. Kourkoumelis, M. Tzaphlidou, Spectroscopic Assessment of Normal Cortical Bone: Differences in Relation to Bone Site and Sex, The Scientific World JOURNAL 10 (2010) 402-412.
[40] J.S. Yerramshetty, C. Lind, O. Akkus, The compositional and physicochemical homogeneity of male femoral cortex increases after the sixth decade, Bone 39(6) (2006) 1236-43.
[41] M.D. Grynpas, R.G. Hancock, C. Greenwood, J. Turnquist, M.J. Kessler, The effects of diet, age, and sex on the mineral content of primate bones, Calcif. Tissue Int. 52(5) (1993) 399-405.
[42] G. Falgayrac, D. Farlay, C. Poncon, H. Behal, M. Gardegaront, P. Ammann, G. Boivin, B. Cortet, Bone matrix quality in paired iliac bone biopsies from postmenopausal women treated for 12 months with strontium ranelate or alendronate, Bone 153 (2021) 116107.
[43] G.S. Mandair, M.P. Akhter, F.W.L. Esmonde-White, J.M. Lappe, S.P. Bare, W.R. Lloyd, J.P. Long, J. Lopez, K.M. Kozloff, R.R. Recker, M.D. Morris, Altered collagen chemical compositional structure in osteopenic women with past fractures: A case-control Raman spectroscopic study, Bone 148 (2021) 115962.
[44] C.M. Weaver, K.M.H. Gallant, Chapter 14 - Nutrition, in: D.B.B.R. Allen (Ed.), Basic and Applied Bone Biology, Academic Press, San Diego, 2014, pp. 283-297.
[45] Y.N. Yeni, J. Yerramshetty, O. Akkus, C. Pechey, C.M. Les, Effect of fixation and embedding on Raman spectroscopic analysis of bone tissue, Calcif. Tissue Int. 78(6) (2006) 363-71.

Raman analysis of skeletal remains

Intrinsic and extrinsic factors

Influence of each factor is mixed in all Raman spectra (X)

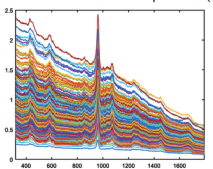

ANOVA-Simultaneous Component Analysis

$$X = X_A + X_B + X_{AB} + E$$

Unmix and separate intrinsic and extrinsic factors

Ranking intrinsic and extrinsic factors

15.66%
Burial Time

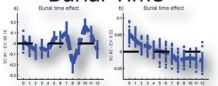

7.54%
Body source